Received: 9 February 2022 | Revised: 19 May 2022 | Accepted: 26 May 2022

DOI: 10.1096/fj.202200215R

THE FASEB JOURNAL

RESEARCH ARTICLE

SNAI1 is upregulated during muscle regeneration and represses FGF21 and ATF3 expression by directly binding their promoters

Ines Elia[1] | **Giulia Realini**[1] | **Vittoria Di Mauro**[2] | **Sara Borghi**[3] | **Laura Bottoni**[1] | **Salvatore Tornambè**[1] | **Libero Vitiello**[4] | **Stephen J. Weiss**[5] | **Mario Chiariello**[6] | **Annalaura Tamburrini**[7,8] | **Salvatore Oliviero**[7,8] | **Francesco Neri**[7] | **Maurizio Orlandini**[1] | **Federico Galvagni**[1]

[1]Department of Biotechnology, Chemistry and Pharmacy, University of Siena, Siena, Italy

[2]IRCCS-Humanitas Research Hospital, Rozzano, Italy

[3]Department of Pathology, NYU Grossman School of Medicine, New York, New York, USA

[4]Department of Biology, University of Padova, Padova, Italy

[5]Division of Genetic Medicine, Department of Internal Medicine, Life Sciences Institute, University of Michigan, Ann Arbor, Michigan, USA

[6]Istituto di Fisiologia Clinica (IFC), Consiglio Nazionale delle Ricerche (CNR) and Core Research Laboratory (CRL), Istituto per lo Studio, la Prevenzione e la Rete Oncologica (ISPRO), Siena, Italy

[7]Department of Life Science and Systems Biology, Università degli Studi di Torino, Turin, Italy

[8]IIGM - Italian Institute for Genomic Medicine, c/o IRCCS, Candiolo, Italy

Correspondence
Federico Galvagni, Department of Biotechnology, Chemistry and Pharmacy, University of Siena, Via A. Moro, 2, 53100 Siena, Italy.
Email: federico.galvagni@unisi.it

Present address
Vittoria Di Mauro, Institute of Genetic and Biomedical Research (IRGB), Milan Unit, National Research Council, Via Fantoli 16/15, Milan, 20138, Italy

Sara Borghi, Immune Monitoring Laboratory, NYU Langone Health, 550 First Avenue, New York, NY 10016, USA

Funding information
Ministero dell'Istruzione, dell'Università e della Ricerca (MIUR)

Abstract

During skeletal myogenesis, the zinc-finger transcription factors SNAI1 and SNAI2, are expressed in proliferating myoblasts and regulate the transition to terminally differentiated myotubes while repressing pro-differentiation genes. Here, we demonstrate that SNAI1 is upregulated in vivo during the early phase of muscle regeneration induced by bupivacaine injury. Using shRNA-mediated gene silencing in C2C12 myoblasts and whole-transcriptome microarray analysis, we identified a collection of genes belonging to the endoplasmic reticulum (ER) stress pathway whose expression, induced by myogenic differentiation, was upregulated in absence of SNAI1. Among these, key ER stress genes, such as *Atf3*, *Ddit3/Chop*, *Hspa5/Bip*, and *Fgf21*, a myokine involved in muscle differentiation, were strongly upregulated. Furthermore, by promoter mutant analysis and Chromatin immune precipitation assay, we demonstrated that SNAI1 represses *Fgf21* and *Atf3* in proliferating myoblasts by directly binding to multiple E boxes in their respective promoter regions. Together, these data describe a new regulatory mechanism of myogenic differentiation involving

Abbreviations: ATF3, activating transcription factor 3; ChIP, chromatin immune precipitation; ER, endoplasmic reticulum; FGF21, Fibroblast Growth Factor 21; MyoD, myogenic differentiation antigen; UPR, unfolded protein response.

the direct repressive action of SNAI1 on ER stress and *Fgf21* expression, ultimately contributing to maintaining the proliferative and undifferentiated state of myoblasts.

KEYWORDS

E box, endoplasmic reticulum stress, gene silencing, microarray analysis, muscle regeneration, myoblast differentiation, promoter, skeletal muscle, transcription

1 | INTRODUCTION

Skeletal muscle development is a complex process that involves myoblast proliferation as well as myofibers differentiation. A molecular switch involving various actors, including myogenic differentiation antigen (MyoD), SNAI1, and SNAI2, regulates the transition from proliferating myoblasts to terminally differentiated myotubes. Members of the SNAI family are zinc-finger transcription factors that recognize and bind to E boxes (5′-CANNTG-3′) with a C/G-rich central dinucleotide and act as transcriptional repressors by recruiting HDAC1/2.[1–3] SNAI1 and 2 are expressed in proliferating myoblasts and rapidly turned off as muscle differentiation proceeds. It has been demonstrated that in proliferating myoblasts, the SNAI1-HDAC1/2 repressive complex is in competition with MyoD, a key regulator of myogenesis, for binding to a subset of G/C-rich differentiation-specific E boxes, thereby preventing the MyoD occupancy on these regulatory elements and consequently blocking terminal differentiation.[4]

Fibroblast Growth Factor 21 (FGF21) is an endocrine hormone expressed in numerous tissues including liver, brown adipose tissue, white adipose tissue, and pancreas.[5] Although the liver is generally considered the main site of FGF21 production, FGF21 may be considered a myokine given that many studies indicate that skeletal muscle can serve as a relevant source of its production, especially in response to insulin stimulation.[6] Moreover, it has been demonstrated that MyoD binds directly to the promoter region of *Fgf21*, leading to the activation of *Fgf21* expression in differentiating mouse C2C12 myoblasts.[7,8] In this cellular context, FGF21 induces the expression of early myogenic genes such as MyoD, MYF4, and MYH1, as demonstrated by overexpression and silencing of FGF21. Moreover, overexpression of FGF21 promotes myoblast cell cycle exit and enhances myogenic differentiation as shown by increased fusion index and myotube length, whereas its negative modulation attenuates these processes.[8,9] In line with these observations, transgenic mice with muscle-specific FGF21 overexpression show decreased muscle mass while both mRNA and protein expression levels of FGF21 are dramatically increased in dystrophic skeletal muscle, underlining its role in muscle development and regeneration in vivo.[8,10]

Independent of these transcriptional events, the endoplasmic reticulum (ER) stress, and ER stress-induced UPR occur transiently during myoblast terminal differentiation and myofiber formation, where they play a critical role in myogenesis.[11–13] ER is a specialized organelle required for its crucial role in the synthesis, assembly, folding, routing, and degradation of a large number of proteins and in Ca^{2+} storage. In response to ER redox imbalance or disruption of ER Ca^{2+} homeostasis, misfolded or unfolded proteins accumulate in the ER,[14] thereby triggering an ER stress response, termed the unfolded protein response (UPR), that serves as a compensatory process that aims to restore ER homeostasis in order to preserve cellular functions and survival.

Activation of UPR pathways is induced by three ER transmembrane sensors: PERK, inositol-requiring protein 1 (IRE1), and activating transcription factor 6 (ATF6).[15–17] In the context of muscle differentiation, IRE1α stimulates skeletal muscle regeneration via a RIDD (regulated IRE1-dependent decay)-mediated decrease in myostatin concentration and impairment of myoblast differentiation.[13] In the early stage of myoblast differentiation, the PERK-ATF4 signaling pathway transactivates muscle differentiation-associated miRNAs, such as miR-128 which promotes myoblast differentiation and inhibits proliferation.[18,19] However, the PERK-ATF4 axis, through CHOP/DDIT3 induction, can also repress MyoD transcription, thereby delaying myoblast differentiation.[20] Lastly, ATF6, but not other ER stress sensors, is specifically activated during apoptosis in myoblasts and promotes myoblast differentiation by enhancing apoptosis of fusion-incompetent cells.[11,12]

To better characterize the role of SNAI1 in myogenesis, we studied the expression of SNAI1 in mouse tibialis anterior muscle following bupivacaine-induced muscle degeneration and regeneration and we identified putative SNAI1 target genes by microarray expression analysis of SNAI1-short hairpin (sh) RNA-silenced C2C12 myoblasts. These studies led to our discovery that SNAI1 represses the ER stress/UPR pathway as well as the expression of the pro-differentiation factor FGF21. Furthermore, by promoter mutation analysis and ChIP, we identified the binding sites for SNAI1 in the promoters of both FGF21 and the ER stress

marker Activating Transcription Factor 3 (ATF3) genes. Together, our data describe a new regulatory mechanism of myogenic differentiation involving the direct repressive action of SNAI1 on ER stress and FGF21 expression, ultimately contributing to maintain the proliferative and undifferentiated states that characterize myoblasts.

2 | MATERIALS AND METHODS

2.1 | Animals and in vivo assays

Animal experiments were performed according to the guidelines for animal experimentation and welfare provided by Padua University and approved by the Padua University ethics committee. For the in vivo analysis, three-month old mice received a pre-emptive dose of the analgesic Carprofen and then were anesthetized with Isoflurane. Skin adjacent to the tibial anterior muscle was shaved, wiped clear of debris with sterile water, and sterilized with alternating scrubs of Iodine/Betadine and alcohol three times. Briefly, 25 µl of bupivacaine 0.5% w/v were injected into the tibialis anterior muscles to induce acute skeletal muscle regeneration through a single intramuscular injection.[21] Following bupivacaine injection, mice were sacrificed at different time points and the tibialis anterior muscles were dissected, frozen, and processed for further analysis.

2.2 | Muscle embedding and cryosectioning

After dissection, skeletal tibialis anterior muscles were embedded with a minimum amount of Tissue-Tek O.C.T (Sakura Finetek, USA). The embedded muscles were frozen by placing them into the cooled 2-methylbutane for 5 min and then the muscle samples were transferred to a −80°C freezer for storage. Ten microliters-thick cryosections were processed for Hematoxylin and Eosin staining.

2.3 | Cell culture, differentiation, and treatment

The C2C12 myoblasts were used as in vitro model for mammalian muscle differentiation.[22] The cells were cultured in Dulbecco's modified Eagle's medium (DMEM) high glucose medium, supplemented with 2 mM L-Glutamine, 100 µg/ml streptomycin, 100 U/ml penicillin, and 20% (v/v) fetal bovine serum (FBS) (Growth medium; GM), at 37°C in a humidified atmosphere containing 5% (v/v) CO_2. To induce myotube differentiation, the C2C12 were cultured in DMEM High Glucose, supplemented with 2 mM L-Glutamine, 100 µg/ml streptomycin, 100 U/ml penicillin, and 2% (v/v) horse serum (HS).[23] The primary mouse satellite cells were cultured in DMEM high glucose supplemented with 2 mM L-glutamine, 100 µg/ml streptomycin, 100 U/ml penicillin 20% (v/v) FBS, 10% (v/v) horse serum, and 1% chicken embryo extract (CEE) at 37°C in a humidified atmosphere containing 5% (v/v) CO_2. All media and solutions for cell culture were purchased from Euroclone (Milan, Italy). Thapsigargin 0.2 µM (Merck KGaA, Darmstadt, Germany) diluted in dimethyl sulfoxide (DMSO) was used to induce ER stress. The control cells were treated with DMSO only. Lenti-X 293T cell line was used to produce lentivirus particles. Lenti-X 293T cells were grown in the DMEM high glucose supplemented with 2 mM L-glutamine, 100 µg/ml streptomycin, 100 U/ml penicillin, and 10% (v/v) FBS, at 37°C in a humidified atmosphere containing 5% (v/v) CO_2. All the cell lines were tested for mycoplasma contamination using MycoAlert Mycoplasma Detection Kit (Lonza, Basel, Switzerland). For the specific inhibition of the ER stress pathways, GSK2656157 (PERK inhibitor; HY-13820, MedChemExpress, NJ, USA), Melatonin (ATF6 inhibitor; HY-B0075, MedChemExpress, NJ, USA), and 4µ8C (IRE1 inhibitor; HY-19707, MedChemExpress, NJ, USA) was used at the final concentration of 10 µM and DMSO was used as a negative control.

2.4 | RNA extraction and RT-qPCR

Total RNA was extracted from C2C12 cells using RNeasy® Plus Mini Kit (Qiagen, Hilden, Germany), according to the manufacturer's instruction. Total RNAs were quantified by QIAxpert system spectrophotometer by measuring the UV/VIS absorption spectrum and used to evaluate the gene expression by means of Brilliant III Ultra-Fast SYBR Green RT-qPCR Master Mix (Agilent Technologies, Santa Clara, CA, USA) was used. Primers for RT-qPCR of mouse genes are shown in Table 1.

2.5 | Western blot analysis

Total cell extracts were prepared as previously described.[24] The protein concentration in each sample was measured using Pierce™ BCA Protein Assay Kit (Thermo Fisher Scientific, Waltham, MA). Primary and secondary antibodies used for immunoblotting are reported in Table 2.

2.6 | Microarray analysis

RNA was exctracted and purified as previously described.[25] Microarray analysis was performed on the

Illumina Platform (Illumina, San Diego, CA, USA) and the results were analyzed using the BeadStudio Gene ExpressionModule (GX). Data were background adjusted and quartile normalized using default parameters in the Genome BeadStudio Software. Probes with p-value $< .05$ in all the three samples of at least one condition were selected for downstream analysis. Differentially expressed (DE) probes were calculated on the Galaxy website (usegalaxy.org) using the Limma package (bioconductor-limma v.3.48.0) with the limma-voom method and Benjamin and Hochberg adjusted p-value (adj$P$) calculation. Differentially expressed probes were defined as adj$P < .05$ and $|\log FC| > 0.5$. Volcano Plot and Heatmaps were generated in Python v3.4.5.

2.7 | Plasmids and site-directed mutagenesis

Based on the mouse *Fgf21* promoter sequence, specific primers were designed (Table 3) to amplify a full-length promoter, spanning from −1764 bp with respect to the transcription start site to +166 bp, and shorter promoter fragments progressively excluding the putative binding sites for SNAI1, previously identified by bioinformatic analysis. In total, four promoter fragments were amplified by PCR from *Mus musculus* genome using the Q5® High-Fidelity DNA Polymerase (New England Biolabs, Ipswich, MA, USA), cloned into the pGL3-Basic vector (Promega Corp., Madison, WI), and named as follows: −1764, −1681, −1091, and −926. The four promoter fragments and the pGL3-Basic vector were digested with KpnI-HF/XbaI and KpnI-HF/NheI-HF restriction enzymes (New England Biolabs, Ipswich, MA, USA), respectively, and then ligated using the T4 DNA ligase (New England Biolabs, Ipswich, MA, USA). The point mutations on the −926 *Fgf21* promoter E-boxes were introduced using the *QuickChange XL Site-Directed Mutagenesis* kit (Agilent, Santa Clara, CA), according to the manufacturer's instructions. The primers used for PCR amplification are listed in Table 4. The primers were designed in order to obtain point mutations of the E-boxes 1, 2, and 3, surrounding the TSS, in the construct

TABLE 1 Primers used for the RT-qPCR analysis

Name	Target gene	5′ > 3′ sequence
O1029	forward *Fgf21*	ACCAAGCATACCCCATCCCT
O1030	reverse *Fgf21*	GCTTCAGTGTCTTGGTCGTCAT
O986	forward *Atf3*	AGACAGAGTGCCTGCAGAAAGA
O987	reverse *Atf3*	TCCGGTGTCCGTCCATTCTGA
N268	forward *Snai1*	TTGGGCCAACTTCCCAAGCA
N270	reverse *Snai1*	AGGAAGGCCTTTCCACAGGT
H237	forward *Gapdh*	GGTCACCAGGGCTGCCATTG
H238	reverse *Gapdh*	TTCCAGAGGGGCCATCCACAG
O611	forward *MyoD*	CGGAGTGGCAGAAAGTTAAGACGA
O612	reverse *MyoD*	AAAAGCGCAGGTCTGGTGAGT
O615	forward *Pax7*	GTTTCCCATGGTTGTGTCTCCAAG
O617	reverse *Pax7*	TTCTGAGCACTCGGCTAATCGAAC
P61	forward *Pdgfa*	GGTGAAGGACAGTGGAGAGTATGA
P62	reverse *Pdgfa*	CTTCGTGCAAGTTGACAGCTTC
O1086	forward *Hgf*	CCCCTTGGGAGTATTGTGCAATTA
O1087	reverse *Hgf*	TGCTTGTGAGGGTACTGCGAAT
O1013	forward *Ddit3/Chop*	ATCCCCAGGAAACGAAGAGGAA
O1014	reverse *Ddit3/Chop*	TGGGCCATAGAACTCTGACTGGAA
O1039	forward *Hspa5/Bip*	CAGCGACAAGCAACCAAAGATG
O1040	reverse *Hspa5/Bip*	CCACCCAGGTCAAACACAAGGAT
O1088	forward *Enpp2*	AGCCTGAATGACTGTGCTGT
O1089	reverse *Enpp2*	TGGGCACTGGGAACCTAGTA
O1069	forward *Angpt1*	TGCCGATTTCAGCACGAAGGAT
O1070	reverse *Angpt1*	TAGATTGGAAGGGCCACAGGCAT
P25	forward *Peg3*	TTCCCAGCAAGGGGAGATCAGTT
P26	reverse *Peg3*	CACTGTTGGTGTCGTCTTCGTGAT

TABLE 2 Primary and secondary antibodies used for western blotting

Primary antibodies	Isotype	Concentration	Source
Anti-ATF3	Rabbit	1:1000	#sc-188X (Santa Cruz Biotechnology, Dallas, TX, USA)
Anti-Histone H3	Rabbit	1:1000	#ab1791 (Abcam, Cambridge, UK)
Anti-Flag M2	Mouse	1:1000	#F3165 (Sigma–Aldrich, Milan, Italy)
Anti-SNAI1	Rabbit	1:1000	#3879 (Cell Signaling, Danvers, MA, USA)
Anti-SNAI2	Goat	1:500	#sc-10437 (Santa Cruz Biotechnology, Dallas, TX, USA)
Anti-MyoD1	Mouse	1:500	#M3512 (DAKO, Milan, Italy)
Anti-MYF4 (Myogenin)	Mouse	1:1000	#sc-12732(Santa Cruz Biotechnology, Dallas, TX, USA)
Anti-p21/WAF1	Rabbit	1:1000	#556430 (BD Pharmingen, Oxford, UK)
Anti- MYH3	Mouse	1:1000	#ALX-805-504 (ENZO Life Sciences, New York, NY)
Anti-PAX7	Rabbit	1:500	#ab34360 (Abcam, Cambridge, UK)
Anti-SNAI2	Rabbit	1:1000	#9585 (Cell Signaling, Danvers, MA, USA)
Anti-FGF21	Rabbit	1:1000	# ab171941 (Abcam, Cambridge, UK)
Anti-DDIT3/CHOP	Rabbit	1:1000	#sc-575 (Santa Cruz Biotechnology, Dallas, TX, USA)
Secondary antibodies	**Isotype**	**Concentration**	**Source**
Anti-rabbit	HRP	1:5000	GE Healthcare Life Science Chicago, IL, USA
Anti-mouse	HRP	1:4000	GE Healthcare Life Science Chicago, IL, USA

TABLE 3 List of oligonucleotides used for the amplification of the Fgf21 promoter region

Fgf21 promoter fragment	Primers for amplification	5′ > 3′ sequence
−1764	Forward A160 Reverse A164	GGGGTACCATGCTCTGGGAGTAGCCACG GCTCTAGACAGGGCTGCGCTCCGTTCGG
−1681	Forward A161 Reverse A164	GGGGTACCGGAGGATGGAGAACCTGTTT GCTCTAGACAGGGCTGCGCTCCGTTCGG
−1091	Forward A162 Reverse A164	GGGGTACCACCCCCCAAAGCATCTGGAG GCTCTAGACAGGGCTGCGCTCCGTTCGG
−926	Forward A202 Reverse A164	GGGGTACCGGGCTGAGGACTCCTCTTACAC GCTCTAGACAGGGCTGCGCTCCGTTCGG

carrying the −926 *Fgf21* promoter. The full length of *Atf3* promoter (−1943) and a deletion fragment excluding putative binding sites for SNAI1 (−1235) were generated by PCR amplification of *Mus musculus* genome (see Table 5 for primer sequences). After the amplification, the PCR products were cloned into pCR®-Blunt II-TOPO®, using the Zero Blunt® TOPO® PCR Cloning kit (Invitrogen-Thermo Fisher Scientific, Waltham, MA, USA). The plasmid constructs were digested with NotI-HF restriction enzyme (New England Biolabs, Ipswich, MA, USA), purified by means of QIAquick PCR purification kit (Qiagen, Hilden, Germany), and blunt ends were generated by means of Large (Klenow) Fragment (New England Biolabs, Ipswich, MA, USA). The fragment Luc+-SV40 late poly(A) signal was obtained by digesting the pGL3Basic vector with XhoI and BamHI (New England Biolabs, Ipswich, MA, USA) restriction enzymes, separated by agarose gel electrophoresis and extracted from the 1% agarose gel. Successively, blunt ends were obtained as above. Then, the fragment Luc+-SV40 late poly(A) signal was inserted into the pCR®-Blunt II-TOPO® promoter constructs by ligase reaction with T4 DNA ligase. The pCMV6 expression vectors for murine Flag-tagged SNAI1 (OriGene Technologies, Inc., Rockville, MD, US) were used in experiments of co-transfection, and the pCMV6-Entry vector was used as control.

2.8 | Cell transfection and luciferase reporter assay

C2C12 cells were seeded at a density of 9×10^4 cells·well^{-1} in a 6-well culture plate and grown for 24 h. For promoter activity tests, 0.8 μg of luciferase reporter vector, 0.4 μg of the pCMV6 expression vector or empty vector, and 0.025 μg of *Renilla* luciferase control vector (pNL1.1 TK[*Nluc*/TK]; Promega) were used for the transfection of a single well with the Attractene Transfection Reagent (Qiagen, Hilden, Germany) in accordance with the manufacturer's

TABLE 4 List of oligonucleotides used for the mutagenesis of the −926 Fgf21 promoter region (substituted nucleotides are underlined)

Fgf21 promoter point-mutant	Primers for amplification	5′ > 3′ sequence
−926 m1	Forward A210	GAACACAATTCCAGCAAGCTTGGCTCCTCAGCC
	Reverse A211	GGCTGAGCAGCCAAGCTTGCTGGAATTGTCTTC
−926 m2	Forward A218	GACAGCCTTAGTGTCTTCTAGACTGGGGATTCAACACAGG
	Reverse A219	CCTGTGTTGAATCCCCAGTCTAGAAGACACTAAGGCTGTC
−926 m3	Forward A208	TCAGGAGTGGGGAGGATCCGTGGGCGGGCCTGT
	Reverse A209	ACAGGCCCGCCCACGGATCCTCCCCACTCCTGA

TABLE 5 List of oligonucleotides used for the amplification of the Atf3 promoter region

Atf3 promoter fragments	Primers for amplification	5′ > 3′ sequence
−1943	Forward A173	GGGGTACCATTTATTCCAGGGCAGCCTG
	Reverse A175	GCTCTAGATTAGCCGATTGGCTCCACTG
−1235	Forward A174	GGGGTACCGCAGTCTGTGCACGTGTAAC
	Reverse A175	GCTCTAGATTAGCCGATTGGCTCCACTG

handbook. After 24 h, the GM was replaced with DM, and the day after, the cells were harvested in Passive Lysis Buffer (Promega Corp., Madison, WI) and the luciferase activity was measured by the Nano Dual-luciferase report™ assay system (Promega Corp., Madison, WI), following the manufacturer's instructions. Luciferase activity was normalized to the activity of the *Renilla* luciferase as an internal control.

C2C12 transfection by electroporation was used to overexpress SNAI1 in order to analyze *Fgf21* and *Atf3* expression. C2C12 cells were trypsinized and 2.0×10^6 cells·point^{-1} were centrifuged three times for 5 min, at 190×*g* with DMEM/F12 supplemented with 2.5% (v/v) FBS and 0.25% (w/v) bovine serum albumin (BSA, Sigma–Aldrich, Milan, Italy). Then, the cells were resuspended in 200 µl of the same medium, and 10 µg of DNA (pCMV6-entry vector or pcMV6-SNAI1) were added. Each mix was put into an electroporation cuvette (Gene Pulser electroporation cuvette, Gap Width 0.2 cm, Bio-Rad; Hercules, CA, USA). Electroporation was performed using the following parameters: 290 V, 1.000 µF, 200 Ω. After the electroporation, the cuvette content was resuspended with pre-warmed complete C2C12 medium and plated in 6-well dishes. After 24 h the GM was replaced with fresh medium and again after 1 day with DM for the other 24 h before luciferase assay.

2.9 | ChIP-qPCR

For the ChIP-qPCR analysis, C2C12 cells transfected with pCMV6 or pCMV6-SNAI1 by electroporation as above and the CUT&RUN Assay Kit (Cell Signaling, Danvers, MA, USA**)** was used following the manufacturer instructions. For the immunoprecipitation, we used the anti-FLAG M2 antibody. Following targeted chromatin digestion by the enzyme pAG-MNase, the reaction was stopped with the Stop Buffer containing digitonin, RNAse A, and Spike-in DNA. The sample normalization spike-in DNA is fragmented genomic DNA from the yeast *S. cerevisiae* that facilitates normalization between samples and between experiments during qPCR analysis.

In the end, input and enriched chromatin samples were collected with the phenol/chloroform extraction followed by ethanol precipitation. The purified, enriched DNA was quantified by qPCR with QuantiTec SYBR Green PCR Master Mix (Qiagen, Hilden, Germany), following the manufacturer's instructions. Oligonucleotides users for qPCR are listed in Table 6. qPCR amplification reaction of spike-in DNA was performed for sample normalization and was analyzed using the Percent Input Method.[26] Signals obtained from each immunoprecipitation were expressed as a percent of the total input chromatin.

2.10 | Snai1 silencing

For the RNA interference-mediated knockdown of SNAI1, we used the lentiviral transfer plasmid pLKO.1 from the TRC shRNA library (Open Biosystems, Huntsville, AL) expressing specific shRNA for mouse SNAI1 (Table 7) or GFP as negative control.[1] Lentiviral particles were produced by transfecting Lenti-X 293T cell line with TransIT-VirusGen Transfection kit (Mirus Bio LLC, Madison, WI) according to the manufacturer's instructions. For each transfection, 1.5 µg of pMD2.VSVG, 2.4 µg of pMDLG/pRRE, and 1.2 µg of pRSV-Rev were mixed and added to 5.1 µg of lentiviral transfer plasmid DNA. At 24 and 48 h post-transfection, supernatants of Lenti-X 293T cells containing the lentiviral particles were transferred in a 50 ml centrifuge

TABLE 6 List of oligonucleotides used for the Fgf21 ChIP-qPCR

locus	Primers for amplification	5′ > 3′ sequence
Fgf21 E-Box Cluster A	Forward A186 Reverse A187	AGATGCTCTGGGAGTAGCCA CGGGGTACGAAGAAGAAGCA
Fgf21 E-Box Cluster B	Forward A190 Reverse A191	GGACGCTGTCTGGTGAAAGA CCTCACCAACCCCTGCTTAG
Fgf21 E-Box Cluster C	Forward A194 Reverse A195	GCTGGGGATTCAACACAGGA AGGGATGGGTCAGGTTCAGA
Fgf21 Exon 2 CTRL	Forward A198 Reverse A199	CTCACCACTGTGGACAGACC AATGACCCCTGGCTTCAAGG
Atf3 E-Box at −1873	Forward A325 Reverse A326	AAAAGATGGGGCAGGTAGGAG GGCACAACCCCGAAGAAAG
Atf3 E-Box Cluster	Forward A321 Reverse A322	CTTTACACCTCAGCGTCCTG GACTGCGGCCCAGGAAT
Atf3 E-Box at −607	Forward A332 Reverse A333	TACGTTAACCCACAGCTGCTA CTCCGATGAATCCACACCGT
Atf3 Exon 1 CTRL	Forward A329 Reverse A330	CATCCATCACTTCTTGTCCCG GCCTCTACGCGGACTTAGG

tube. The medium was filtered by using 0.45 μm filters, aliquoted, and stored at −80°C. For C2C12 transduction, the cells were plated in 6-well plates at a concentration of 9.6×10^4 cells per well. After 24 h, the culture medium was replaced with 1 ml of complete C2C12 medium, 1 ml of Lenti-X 293T supernatant containing lentiviral particles and 2 μg of polybrene (hexadimethrine bromide, Sigma–Aldrich, Milan, Italy), per well. After 24 h, medium was changed, and after other 48 h, cell extracts were analyzed by western blot or transcriptome.

2.11 | Statistical analysis

The data analysis was performed using Prism 9 statistical software (GraphPad Software Inc., San Diego, CA). Significance was estimated by one-way or two-way ANOVA. The significant differences were estimated using Tukey's multiple comparison test (*$p < .05$; **$p < .01$; ***$p < .001$; ****$p < .0001$, n.s., not significant). Student's *t* test was used to confirm significant differences between treatments. Two-tailed probabilities of less than .05 were considered significant.

3 | RESULTS

3.1 | SNAI1 is upregulated during early stages of skeletal muscle regeneration and in proliferating C2C12 myoblasts

While SNAI1 has been reported to be expressed in proliferating myoblasts in vitro,[4] we sought to evaluate the expression profile of SNAI1 during myogenesis in vivo. As such, a mouse model of myotoxin-induced muscle degeneration was used, i.e., bupivacaine-induced muscle injury, that serves as a useful in vivo experimental model for studying factors involved in muscle differentiation and muscle plastic adaptation to functional demand.[21] In this model, regeneration requires the activation of undifferentiated satellite cells, which proliferate, differentiate into myoblasts expressing muscle-specific markers, fuse into myotubes, and finally mature into myofibers.[21] Briefly, bupivacaine was injected in the mouse tibialis anterior muscles, with tissues collected at different stages of muscle regeneration for mRNA and protein content analyses. After bupivacaine injection, proliferation of mononuclear cells, mainly inflammatory, and myogenic cells, was most active within 1–4 days of injection.[27] Myogenic cell differentiation and new myotube formation were observed ~5–6 days post injection. Ten days after the injection, the overall architecture of the muscle was restored, although most regenerated myofibers were smaller and displayed central myonuclei (Figure 1A). SNAI1 mRNA and protein were induced early in regenerating muscle (2–4 days after the injury), corresponding with the maximum activation of satellite cells, as defined by MyoD expression (Figure 1B,C). SNAI1 mRNA expression rapidly decreased at day 6, coinciding with the beginning of the myotubes differentiation program, as defined by the increased expression of embryonic skeletal muscle myosin heavy chain (MYH3) and concurrent decline of MyoD expression, supporting a potential role for SNAI1 during the early stages of muscle regeneration. Similarly, SNAI2 was maximally induced at day 3 after the injury, but its expression was maintained up to day 10 (Figure 1B).

shRNA	ID clone TRC	5′ > 3′ sequence
shRNA-1	TRCN0000096619	GCCACCTTCTTTGAGGTACAA
shRNA-2	TRCN0000096620	CCACTCGGATGTGAAGAGATA
shRNA-3	TRCN0000096622	GCAAATATTGTAACAAGGAGT

TABLE 7 List of shRNA used for the mouse SNAI1 knockdown

In primary skeletal myoblasts, SNAI1 is known to repress genes upregulated during muscle terminal differentiation with SNAI1 knockdown leading to the precocious cell cycle withdrawal and terminal differentiation.[4] To define the role of SNAI1 during earlier stages of myogenic differentiation, we used the C2C12 cell line as a widely used and well-established in vitro model for studying mammalian muscle differentiation. Additionally, in the presence of growth factors, these cells are considerably less prone to spontaneous differentiation than primary myoblasts, a feature that optimizes their use as a model to study the transcriptome of proliferating myoblasts. This is confirmed by the lower expression levels of p21 (CIP1/WAF1), a key inducer of cell-cycle arrest, and myogenin (MYF4) under growth conditions (Figure 1D,E). SNAI1 was expressed in proliferating C2C12 cells maintained in a growth medium and was rapidly downregulated after switching to a low-serum differentiation medium (Figure 1D), showing an expression profile that resembles that obtained with primary myoblasts (Figure 1E).[4] SNAI1 mRNA expression profile did not correlate with the protein levels (Figure 1F), however, suggesting a post-translational regulatory mechanism underlying its downregulation during myoblasts-to-myotube differentiation. Indeed SNAI1 is a short-lived protein since it is rapidly ubiquitinated and degraded by the 26S proteasome system. Its degradation is triggered by phosphorylation, such as that mediated by protein kinase 1D (PKD1), a kinase rapidly upregulated during myoblast differentiation or by GSK-3β.[28,29] Moreover, with regard to discrepancies between SNAI1 mRNA and protein expression, SNAI1 can also act as a repressor of its own promoter via a negative feedback loop.[30] Similarly, SNAI2 was expressed in proliferating myoblasts and rapidly downregulated after switching to a differentiation medium (Figure 1E). Conversely, in C2C12 cells, the SNAI2 protein shows a different expression profile with an increased expression on day 1 after switching to a differentiation medium and a more persistent expression that could explain why this cell line is less prone to differentiation (Figure 1D).

3.2 | Silencing of SNAI1 affects ER stress- and cell proliferation-related gene expression in C2C12 myoblasts

To identify genes regulated by SNAI1 in proliferating myoblasts, C2C12 cells were transduced with lentiviral particles for the expression of three different small hairpin RNAs (shRNA) in order to downregulate SNAI1 expression. A substantial reduction of SNAI1 protein level was observed in all three shRNAs (Figure 2A). When cultured in a growth medium, the SNAI1-silenced C2C12 cells did not show alterations in the proliferation rate or spontaneous differentiation to myotubes (Figure S1). Microarray gene expression profile analysis was performed with mRNA extracted from C2C12 cells (Table S1) and 180 significantly downregulated and 218 significantly upregulated genes were found in all three SNAI1 knockdown cell lines as compared with control transduced cells (adj$P < .05$ and $|\log FC| > 0.5$) (Table S2 and Figure 2B,C). To begin defining the biological categories affected by SNAI1 silencing, the differentially expressed genes (DEGs) were subjected to gene ontology (GO) enrichment analysis performed using the online Database for Annotation, Visualization, and Integrated Discovery (DAVID) analysis platform (Table S3).[31] To identify only the context pertinent and non-redundant enriched GO terms in biological processes, a selected list of significantly enriched terms (p-value $< .05$) was plotted using REVIGO.[32] This analysis identified two main biological processes significantly enriched in this gene set both as p-value and number of DEG; endoplasmic reticulum (ER) stress (GO:0034976 and GO:0030968; ER stress and UPR are closely related processes) and positive regulation of cell proliferation (GO:0008284) (Figure 2D–F). Changes in gene expression were validated by real-time quantitative PCR (RT-qPCR) for a selected group of genes, including *Fgf21, Atf3, DNA damage-inducible transcript 3 protein* (*Ddit3*), *heat shock protein family A* (*Hsp70*) *member 5* (*Hspa5/Bip*), *hepatocyte growth factor* (*Hgf*), *ectonucleotide pyrophosphatase/phosphodiesterase 2* (*Enpp2*), *and platelet-derived growth factor receptor alpha (Pdgfra)* (Figure 2G). As expected, DAVID analysis did not identify pathways involved in myoblast terminal differentiation, confirming that the ability of C2C12 to maintain an undifferentiated phenotype in high serum conditions is not dependent on SNAI1 expression even though the expression of a large group of genes involved in cell proliferation is perturbed.

3.3 | SNAI1 represses FGF21 and ATF3 expression in proliferating myoblasts by directly interacting with their gene promoters

As during myogenesis, SNAI1 acts as a transcriptional repressor,[4] we focused our attention on shRNA upregulated

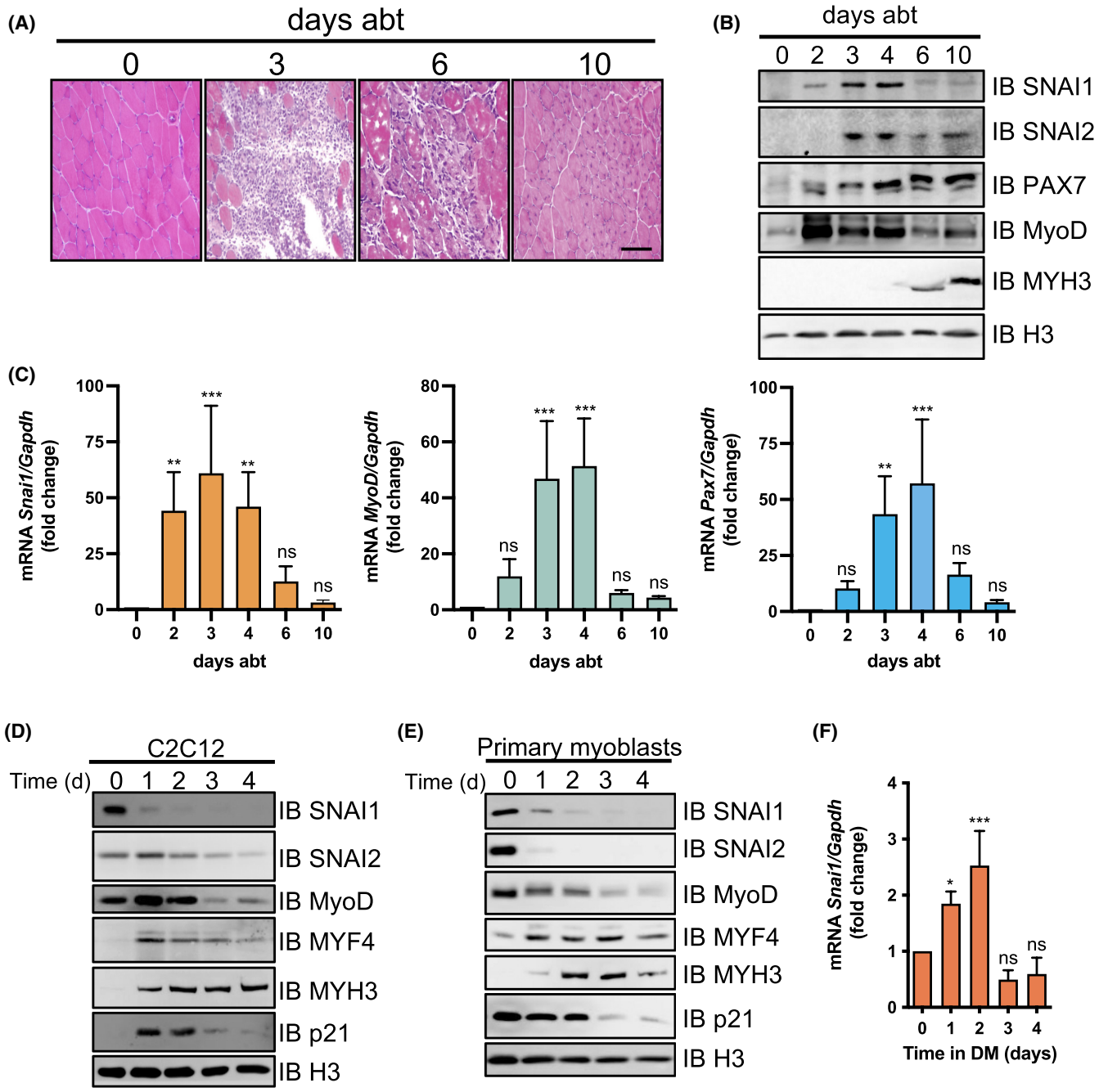

FIGURE 1 Expression of SNAI1 protein and mRNA during muscle regeneration and myoblasts differentiation. (A) Eosin–hematoxylin staining of cross-sections from tibialis anterior muscles at day 0 (untreated), 3, 6, and 10 days after bupivacaine treatment (abt). Bar, 50 μm. (B) Snai1 protein expression was detected by western blot analysis of whole extracts prepared from regenerating muscles at the indicated days abt. Histone H3 expression was used to confirm equal loading. PAX7, MyoD, and MYH3 expression was detected as control of satellite cell-derived myoblasts proliferation (PAX7 and MyoD) and differentiation (MYH3). (C) Quantitative evaluation of *Snai1* transcript in regenerating muscle by RT-qPCR. *MyoD* and *Pax7* transcripts were measured as muscle regeneration control. The values normalized to the glyceraldehyde-3-phosphate dehydrogenase (*Gapdh*) mRNA levels are expressed as the mean ± SD of 3 independent experiments. Asterisks indicate significant differences (*p*-values) between expression in untreated muscle (0) and each other time point. Snai1 protein expression was detected by Western blot analysis of whole-cell extracts prepared from proliferating and differentiating C2C12 cells (D) and primary mouse myoblasts (E). Time (d) indicates the days after switching to differentiation medium (DM). Histone H3 expression was used to confirm equal loading. MyoD, MYF4, and MYH3 expressions were detected as control of myoblasts differentiation. $p21^{WAF1/Cip}$ (p21) was used as a marker of cell cycle arrest. (F) Quantitative evaluation of *Snai1* transcript by RT-qPCR during C2C12 differentiation. The values normalized to *Gapdh* mRNA levels are expressed as the mean ± SD of 3 independent experiments. Asterisks indicate significant differences (*p*-values) between expression at day 0 and each other time point after switching to DM.

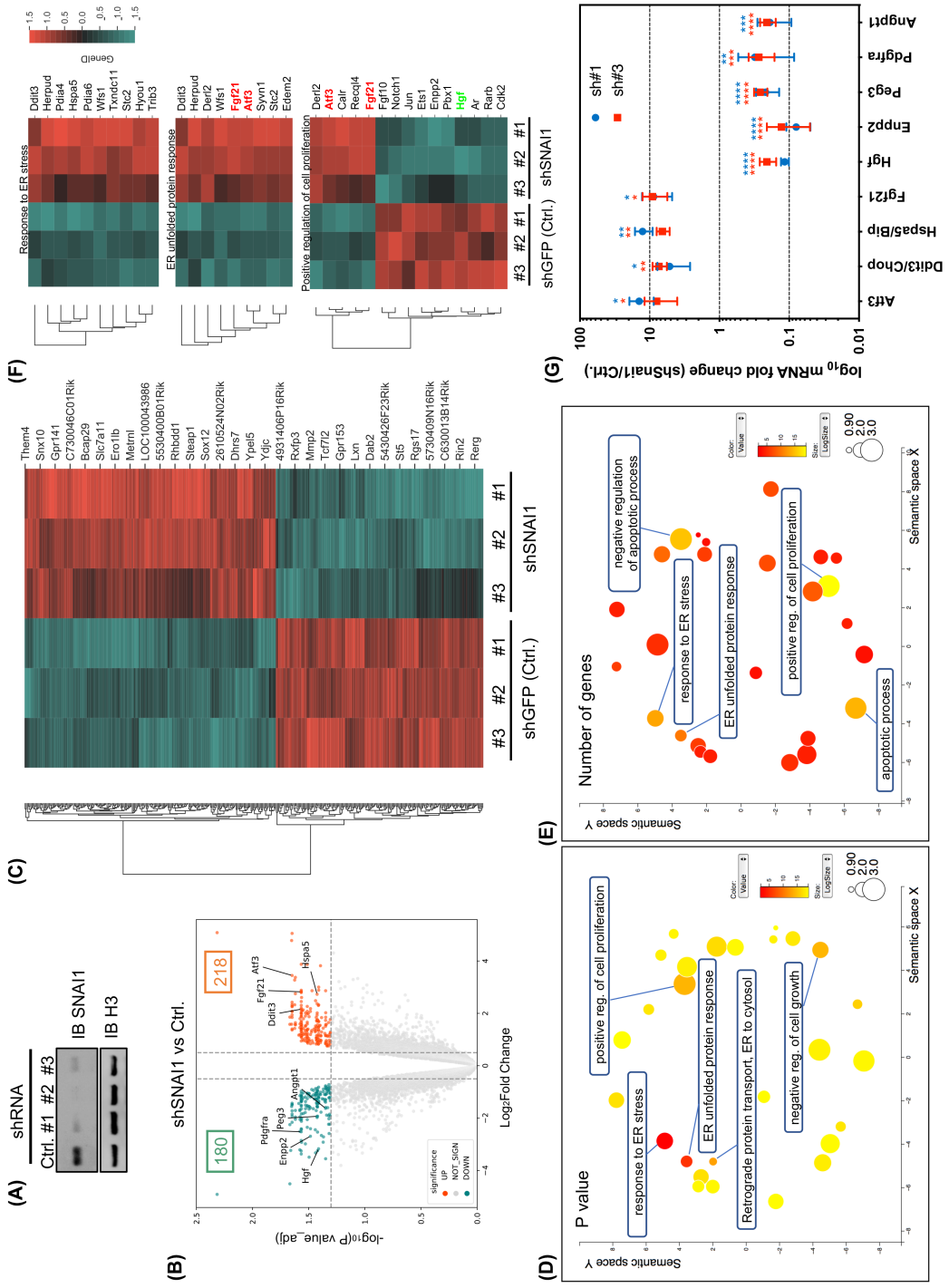

FIGURE 2 Transcriptome analysis of C2C12 myoblasts silenced for SNAI1 knockdown in proliferating C2C12 myoblasts. (A) SNAI1 expression was silenced in C2C12 cells by transduction of lentiviral vectors expressing three different shRNAs. Control cells were infected with a lentiviral vector expressing shRNA for GFP (Ctrl.). RNA samples were used for microarray gene expression analysis. (B) Volcano plot and (C) heatmap revealed differentially expressed genes between control and Snai1 silenced cells. The genes validated by RT-qPCR are indicated in the volcano plot. (D, E) Gene ontology analysis was performed to identify a biological process for differentially expressed genes and context pertinent and non-redundant enriched GO terms in biological processes were plotted using REVIGO. GO terms are represented by circles and are clustered according to semantic similarities to other GO terms in the gene ontology (more general terms are represented by larger size circles, and adjoining circles are most closely related). Bubble colors indicate log10 *p*-value (D) or the number of DEG in the GO term (E). The top five statistically most significant (D) and most gene-rich (E) GO terms are specified. (F) Heatmaps of the three GO terms in common between scatter plots D and E. (G) RT-qPCR was performed to validate the expression increases of *Atf3*, *Ddit3*, *Hspa5*, and *Fgf21*, and the decreases of *Hgf*, *Enpp2*, *Peg3*, *Pdgfra*, and *Angpt1*. Results were normalized to *Gapdh* mRNA. Mean values from three independent experiments are shown with standard deviations.

genes in order to identify new target genes. Among two of the most upregulated transcripts were *Fgf21* and *Atf3*. During muscle cell differentiation, *Fgf21* is positively regulated by the transcription factor MyoD, thereby activating the expression of early myogenic genes, promoting cell cycle exit, and enhancing myogenic differentiation.[9] In turn, ATF3 is a well-known marker of ER stress activation,[33] a response required for early myoblast differentiation. Given SNAI1 expression during myogenesis and the effect of FGF21 and ER stress response on myogenic differentiation, we first examined their expression pattern during muscle regeneration in vivo. In bupivacaine-treated muscle, both FGF21 and ATF3 mRNA and protein were strongly induced (Figure 3A–D). In this experimental model, SNAI1 expression was partially overlapping with FGF21 and ATF3 expression. Nevertheless, these data may remain consistent with the repressive role of SNAI1 on these genes as myoblasts are only partially synchronized in their differentiation process. Indeed, when the expression of FGF21 and ATF3 mRNA were monitored in synchronized C2C12 cultures, following the switch to a low serum medium their expression was strongly induced, as opposed to the fall in SNAI1 protein expression as well as in mRNA expression of two of the most downregulated genes following SNAI1 silencing, *Hgf*, and *Pdgfra* (Figure 3E–G). Moreover, ectopic overexpression of SNAI1 in differentiating myoblasts induced a consistent decrease of both FGF21 and ATF3 mRNA levels, thereby confirming the role of SNAI1 in their negative regulation (Figure 4A–C).

In an effort to characterize the promoter regions that might be involved in this regulation, we performed a bioinformatic analysis that identified the potential E box binding sites for SNAI1 (CACCTG, CACGTG, and CAGCTG) in the mouse *Fgf21* promoter region sequence. Three clusters of putative SNAI1 binding sites were centered on positions −1659 (cluster A), −1000 (cluster B), and +21 (cluster C) with respect to the transcriptional start site (TSS; +1). To determine the functional activity of these E boxes relative to SNAI1 binding, we generated luciferase reporter constructs carrying *Fgf21* promoter regions of different lengths, spanning from position +166 to −1764, −1681, −1091, and −926 (Figure 5A), and the reporter vectors were co-transfected together with pCMV6-SNAI1 expression vector or a pCMV6-empty control vector in C2C12 myoblasts. In this system, both the full length and each of the 3 other promoters with progressive 5′ deletions decreased their activity when SNAI1 was overexpressed, but the full length −1764 promoter proved to be the most responsive to the repression by SNAI1 (Figure 5B,D). To investigate which E boxes contained in cluster C are directly bound by SNAI1, we introduced single and multiple point mutations altering the nucleotide sequence of one, two, or all the three E boxes in the reporter vector harboring the −926 promoter. We observed that only the triple point-mutant was no longer responsive to SNAI1 repressive activity (Figure 5C,D), suggesting that all three binding sites play a role in SNAI1 recruitment to the *Fgf21* promoter. To further verify and characterize the direct binding of SNAI1 to the *Fgf21* promoter, ChIP followed by qPCR was performed in C2C12 cells transiently transfected for the expression of Flag-tagged SNAI1. As shown, SNAI1 effectively binds to the *Fgf21* promoter and the E box clusters interested are the cluster A and C, but not B. No significant signal increase was observed with primers annealing in exon 2 sequence that was used as a negative control (Figure 5E). Similar analyses performed for the *Atf3* promoter demonstrate the binding of SNAI1 to E boxes located at −1873 and between −1320 and −1221 with respect to the TSS (Figure 6).

As FGF21 expression can be induced both by ER stress[34,35] and the transactivation action of MyoD, SNAI1 could serve to repress FGF21 expression mediated by ER stress stimuli other than those associated with myoblast differentiation programs per se. To test this hypothesis, C2C12 cells were treated with thapsigargin, a well-characterized ER stress-inducing agent, and FGF21 mRNA expression was measured at different time points. The results showed an induction of the level of FGF21 mRNA in cycling C2C12 cells as a consequence of the ER stress induction (Figure 7A). Finally, C2C12 cells were transiently co-transfected with the −1764 *Fgf21* promoter reporter plasmid and pCMV6-empty vector or pCMV6-SNAI1 to overexpress SNAI1. After 24 h from the transfection, cells were treated with thapsigargin. Measurement of luciferase activity showed that *Fgf21* promoter activity was upregulated in response to the thapsigargin treatment and SNAI1 was able to repress this induction (Figure 7B). Moreover, using specific inhibitors of the three ER stress pathways, we find that in differentiating myoblasts, FGF21 transcription is downstream of the IRE1 pathway, while ATF3 and DIDIT3/CHOP expression depend on the PERK-ATF4 axis (Figure 7C–E). In addition, we analyzed the myoblast differentiation by means of western blot analysis of MYH3 expression in C2C12 cells treated with the ER stress inhibitors. As shown in Figure 7F, ATF6 and IRE1 pathways, but not the PERK-ATF4 axis, are involved in the promotion of myoblast differentiation.

4 | DISCUSSION

Skeletal muscles possess a unique ability to regenerate completely the following damage. After acute injury or trauma, degeneration is induced, followed by regeneration processes that involve different cell populations,

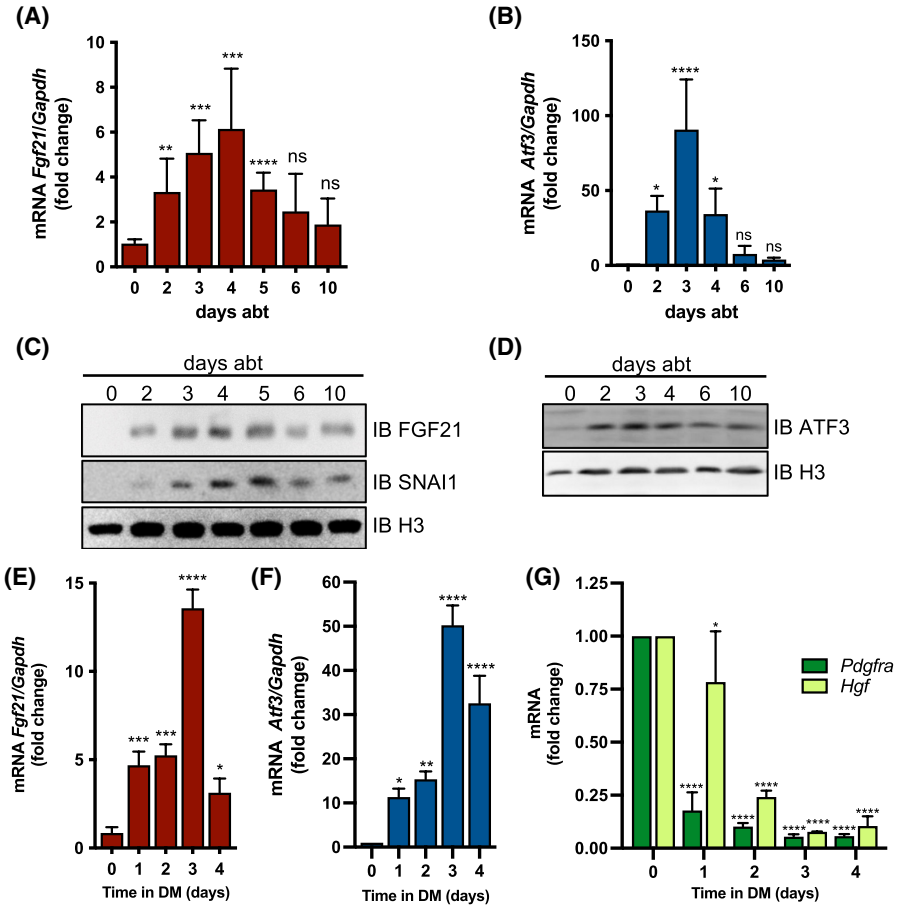

FIGURE 3 FGF21 and ATF3 mRNA and protein expression are upregulated during muscle regeneration and myoblast differentiation. Quantitative evaluation of FGF21 (A) and ATF3 (B) mRNA by RT-qPCR during muscle regeneration. Asterisks indicate significant differences (*p*-values) between expression in untreated muscle (0) and each time point. FGF21 (C) and ATF3 (D) protein expression were detected by Western blot analysis in whole extracts prepared from regeneration muscle at the indicated days abt. Histone H3 expression was used to confirm equal loading. Quantitative evaluation of FGF21 (E), ATF3 (F), HGF, and PDGFRA (G) mRNA by RT-qPCR during C2C12 differentiation. Asterisks indicate significant differences (*p*-values) between expression at day 0 and each time point. The normalized values are the mean and standard deviation from three to six independent experiments.

including a resident population of muscle cell progenitors, i.e., satellite cells. In the absence of environmental stimuli, satellite cells that are located in a specialized niche between the sarcolemma and the basal lamina are maintained in a quiescent state. Following injury or in various disease states, satellite cells are activated, proliferate, and migrate to the damaged areas, where they eventually differentiate, giving rise to newly formed myofibers.[36] Our data show that in vivo, during the muscle degeneration-regeneration process induced by bupivacaine, the transcriptional repressor, SNAI1, is upregulated, both at the protein and mRNA levels, at 3–4 days post-injury when quiescent satellite cells are activated and assume a proliferative state, confirming its possible involvement as a negative regulator in the muscle differentiation process. In this process, the MRFs such as MyoD, MYF4, MYF5, and MRF4 are later engaged where they play a crucial role in committing satellite cells to terminal differentiation.[37]

To prevent premature differentiation, SNAI1 and SNAI2 compete with MyoD for the same binding sequences and act as terminal differentiation repressors by recruiting HDAC1/2 to target genes.[3,4] To gain further insight into the specific role that SNAI1 plays during myogenesis and to identify new SNAI1 target genes, we silenced SNAI1 in the C2C12 myoblast cell line. As opposed to primary myoblasts,[4] C2C12 cells do not terminally differentiate in the presence of growth factors, and as a consequence of SNAI1 knockdown, maintain a proliferative rate similar to that of control cells. As such, these cells serve as an optimal model to study SNAI1-dependent effects on the transcriptome of a pure population of proliferating myoblasts. Using three different shRNAs to avoid silencing artifacts, we identified almost 400 DEGs. The relatively low number of DEGs identified is explained by the selectivity of the analysis performed and also by the partially overlapping repressor activities of SNAI1 and SNAI2, which allowed

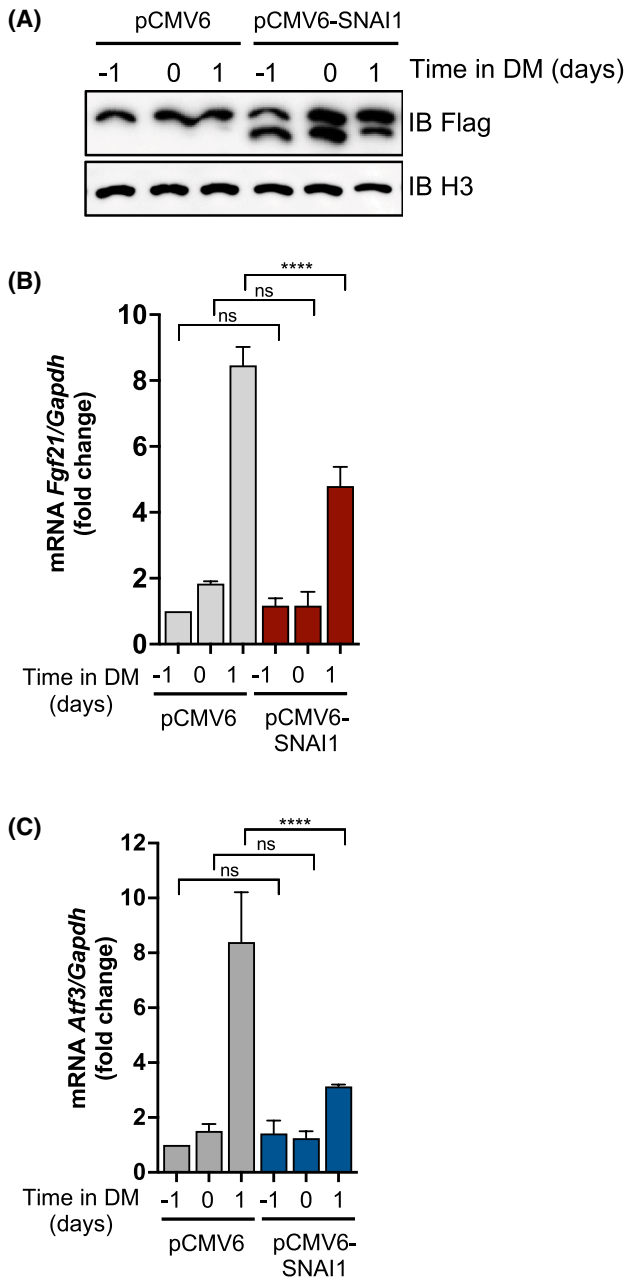

FIGURE 4 FGF21 and ATF3 expression was repressed by overexpression of SNAI1 in differentiating myoblasts. (A) C2C12 myoblasts were transiently transfected with the pCMV6-emty plasmid or with the pCMV6-SNAI1 plasmid and exogenous SNAI1 protein expression was detected by Western blot analysis by means of anti-FLAG antibody. Myoblasts differentiation was induced 48 h post-transfection by the medium switch, which corresponds to day 0 of differentiation. Histone H3 expression was used to confirm equal loading. *Fgf21* (B) and *Atf3* (C) expression was analyzed by RT-qPCR at 24, 48, and 72 h after transfection corresponding to differentiation day −1, day 0, and day 1, respectively. The values were normalized to the *Gapdh* mRNA levels. Asterisks indicate significant differences (*p*-values) between expression in control (pCMV6) and SNAI1 overexpressing (pcMV6-SNAI1) C2C12 cells at the indicated days after the switch to differentiation medium. Data were evaluated from three independent experiments using the one-way analysis of variance ANOVA.

us to identify the subset of genes regulated exclusively by SNAI1. In proliferating C2C12 cells, SNAI2 is likely sufficient to maintain the undifferentiated phenotype, a conclusion consistent with the more stable expression of SNAI2, compared with primary myoblasts (Figure 1D,E), and the absence of enriched GO terms related to myoblast terminal differentiation after SNAI1 silencing.

ER stress, the UPR, and regulation of cell proliferation were the main biological processes identified as significantly enriched by DAVID analysis following SNAI1 targeting. Among cell proliferation-related genes, two of the most downregulated genes were *Hgf* and *Pdgfra*, whose expression during myoblasts differentiation was inversely related to SNAI1 expression. Interestingly, it has been described that HGF released during muscle repair promotes the quiescent satellite cells to enter the cell cycle while inhibiting muscle cell differentiation by positively regulating the expression of the myogenic-inhibitory transcription factor, Twist1, which negatively regulates the cell-cycle inhibitor, p27.[38,39] Furthermore, in vitro studies have described an autocrine loop involving HGF and its receptor, c-met, wherein signaling results in the silencing of MyoD and MYF4 gene expression, thereby inhibiting myotube formation.[40] Similarly, PDGFRα signaling can impair terminal myogenic differentiation in C2C12 cells[41] while other genes downregulated following SNAI1 silencing, such as *Notch1*, *Androgen receptor* (*Ar*), *Cdk2*, *Peg3*, *c-Jun*, and *Rarb*, are also known to promote myoblast proliferation and inhibit myotube differentiation.[42–47] These observations suggest that SNA1 inhibits myoblast differentiation by indirectly promoting the expression of genes involved in myoblast proliferation. Interestingly, another gene belonging to the GO term "regulation of cell proliferation," is *Fgf21*, which in a contrary fashion, is upregulated in SNAI1 knockdown cells. However, FGF21 is an atypical member of the FGF family and, in addition to its function as a regulator of energy metabolism, is significantly increased under certain conditions, such as muscular dystrophy[48] and exercise.[49] Furthermore, in the context of myoblast differentiation, *Fgf21* is a direct transcriptional target of MyoD, which activates the expression of the early myogenic genes, promotes cell cycle exit, and enhances myogenic differentiation.[8,9,50] Here, we described for the first time that FGF21 is upregulated, both as mRNA and protein, in vivo during muscle regeneration, supporting its potential role in the regulation of myogenic differentiation. Interestingly, FGF21 inhibits macrophage-mediated inflammation by activating NRF2 and suppressing the NF-κB signaling pathway[51] while promoting anti-inflammatory M2 macrophage polarization.[52]

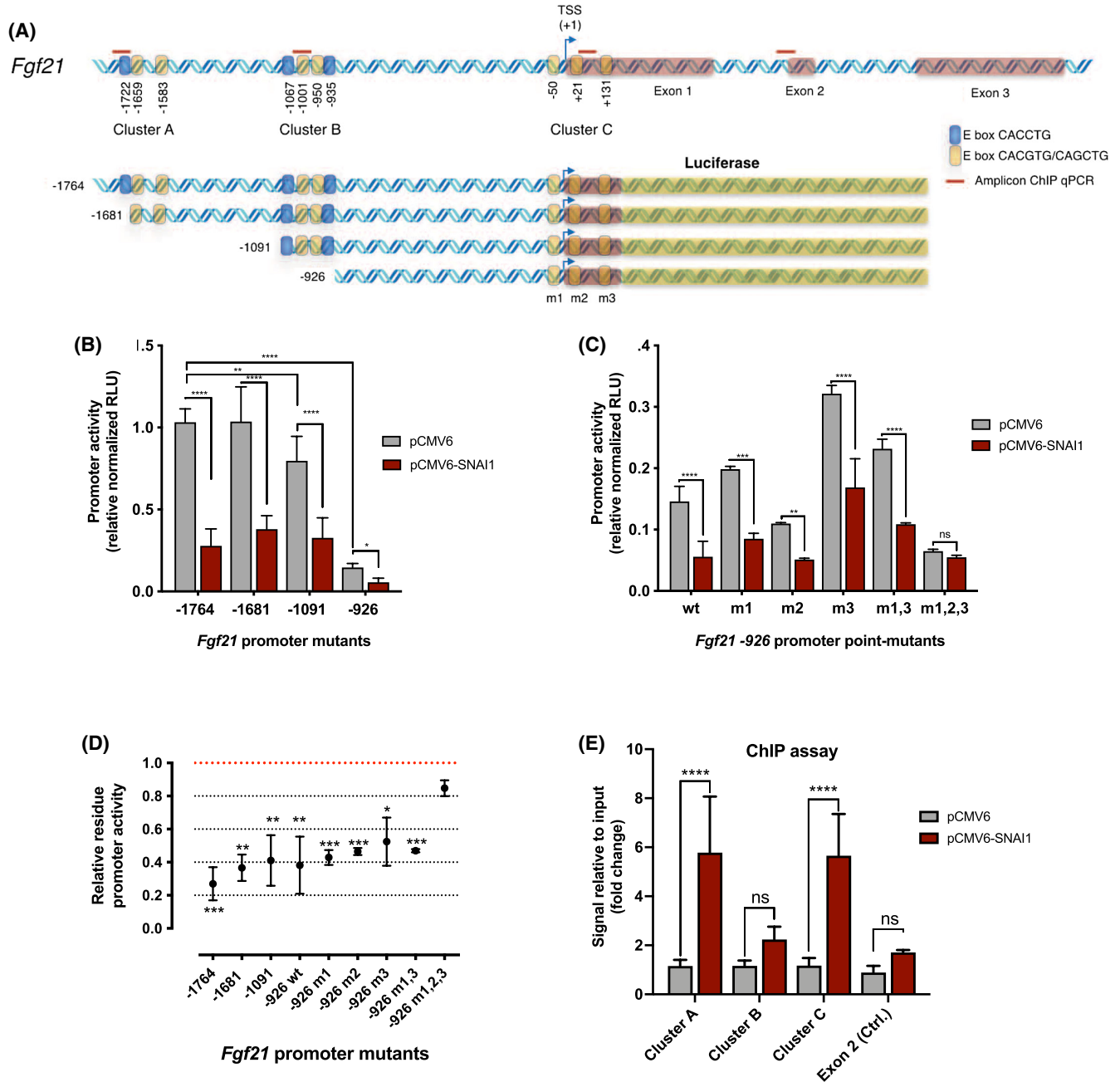

FIGURE 5 SNAI1 regulates *Fgf21* promoter activity by binding directly to E box sequences. (A) Schematic representation of the *Fgf21* gene and the four promoter fragments, which were cloned upstream of the luciferase reporter gene. The blue and yellow boxes represent the E Box CACCTG and CACGTG/CAGCTG, respectively. Positions of the identified E boxes with respect to the TSS are indicated and referred to the first bp of the CANNTG consensus. The E boxes are grouped into three clusters. Point mutations of cluster C E boxes are referred as to m1, m3, and m3. The amplicon obtained after ChIP-qPCR is represented as red lines. Pink boxes represent the exon sequences. (B, C) C2C12 myoblasts were transiently co-transfected with the pCMV6-emty or with the pCMV6-SNAI1 plasmid and the reporter plasmids carrying the indicated *Fgf21* promoter fragments (B) or E box point mutants of the −926 promoter fragment (C). Luciferase activity was assayed 24 h after the switch to DM and normalized to the *Renilla* luciferase internal control and expressed as fold change relative to cells co-transfected with the plasmid carrying the full length (−1764) promoter and the pCMV6-emty vector. (D) SNAI1 transcription factor repressive activity is here expressed as relative residue activity of each promoter mutant obtained by normalizing luciferase activity of cells co-transfected with pCMV6-SNAI1 to that of cells co-transfected with empty control vector. *p*-Values represent statistical differences between the relative residue activity of each promoter and the relative residue activity of the promoter −926 carrying point mutations of all three E boxes of cluster C (−926 m1,2,3). (E) SNAI1 binds both E box clusters A and C in the *Fgf21* promoter region. pCMV6-SNAI1 or empty control vectors were transiently co-transfected in C2C12 and ChIP assay with anti-FLAG antibody followed by qPCR was performed. Upon normalization to spike-in DNA, results were expressed as a signal relative to input. Data were evaluated from three independent experiments using the two-way (B, C, and E) and one-way (D) ANOVA.

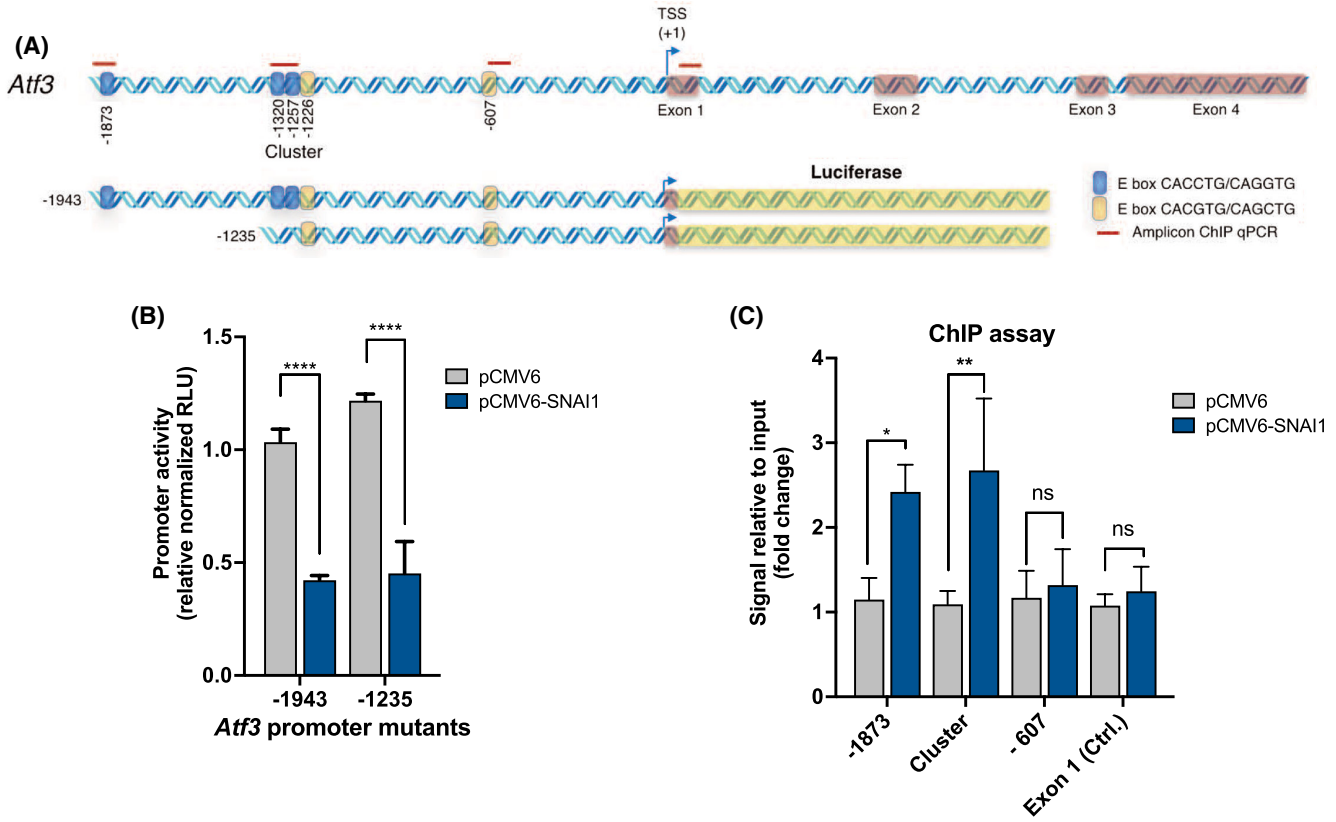

FIGURE 6 SNAI1 regulates *Atf3* promoter activity by binding directly to E box sequences. (A) Schematic representation of the *Atf3* gene and the two promoter fragments, which were cloned upstream of the luciferase reporter gene. (B) C2C12 myoblasts were transiently co-transfected with the pCMV6-emty or with the pCMV6-SNAI1 plasmid and the reporter plasmids carrying the indicated *Atf3* promoter fragments. Luciferase activity was assayed 24 h after the switch to DM and normalized to the *Renilla* luciferase internal control and expressed as fold change relative to cells co-transfected with the plasmid carrying the full length (−1943) promoter and the pCMV6-emty vector. (C) SNAI1 binds both E box at −1873 and the E box cluster centered at −1270. pCMV6-SNAI1 or empty control vectors were transiently co-transfected in C2C12 and ChIP assay with anti-FLAG antibody followed by qPCR was performed. Upon normalization to spike-in DNA, results were expressed as a signal relative to input. Data were evaluated from three independent experiments using two-way ANOVA.

Macrophages massively infiltrate muscle injury sites and participate in the skeletal muscle regeneration process.[53–57] Pro-inflammatory monocytes recruited after skeletal muscle injury stimulate myogenic cell proliferation, but later transition into an anti-inflammatory state that supports myogenesis by promoting myoblast terminal differentiation.[58,59] Taken together, these findings allow us to speculate that myoblast-derived FGF21 promotes myogenic differentiation both by acting directly on myoblast cells and indirectly promoting macrophage switching from a pro-inflammatory M1 to anti-inflammatory M2 phenotype.

In considering additional genes upregulated in response to SNAI1 silencing, we also found *Atf3*, *Ddit3/Chop*, and *Hspa5/Bip*, transcripts coding for key molecules linked to ER stress and ER UPR-related processes.[60–62] Similarly to what we observed for FGF21, we find that ATF3 is upregulated during muscle regeneration in vivo and myoblast differentiation in vitro when SNAI1 expression decreases. Furthermore, we found that in differentiating myoblasts, SNAI1 overexpression downregulates *Fgf21* and *Atf3* transcripts and negatively regulates their promoter regions wherein SNAI1 binds multiple E boxes organized in clusters. However, due to methodological limitations, we are not able to discriminate among the E boxes recognized by SNAI1within the same cluster as they are confined to a DNA region less than 200 bp in size, and the resolution limit of the chromatin complexes cleaved by the pAG-Mnase. In any case, the fact that the basal activity of the full-length *Fgf21* promoter decreased drastically in the −926 deletion mutant is in agreement with the observation presented by Liu et al.[9] where they have described the first E box of the cluster B in position −1067 as a binding site for the transactivator, MyoD, and an essential element for the full promoter activity. In our study, SNAI1 binding sites did overlap with the MyoD-targeted

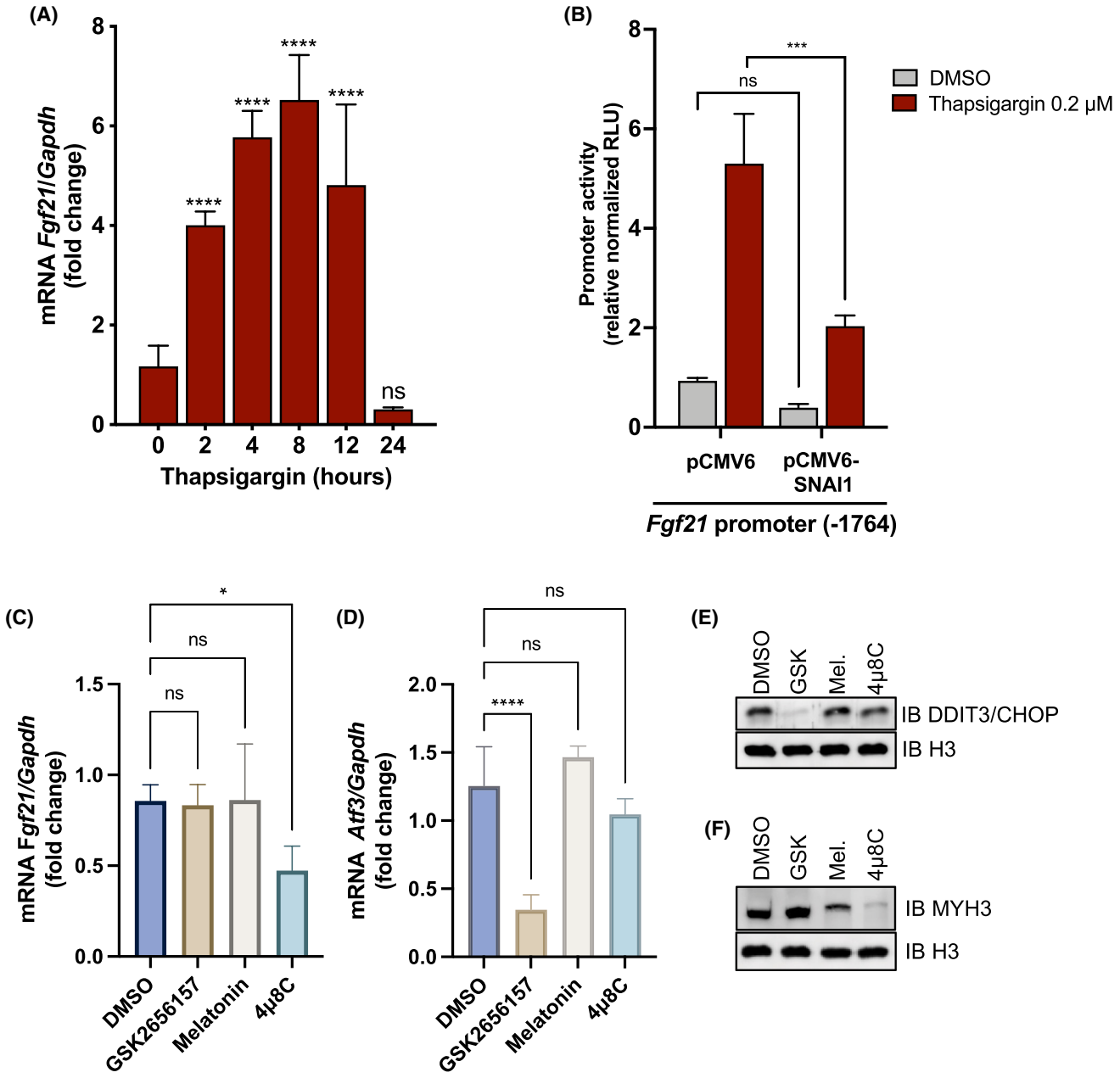

FIGURE 7 SNAI1 represses *Fgf21* promoter activity induced by ER stress. (A) The ER stressor thapsigargin induces the expression of *Fgf21* mRNA in myoblasts. RT-qPCR was performed on RNA extracted from C2C12 myoblasts treated with DMSO (day 0) or with 0.2 µM thapsigargin at different time points. Asterisks indicate significant differences (*p*-values) between expression at day 0 and each time point. (B) Thapsigargin-induced *Fgf21* promoter activity is repressed by overexpression of SNAI1. C2C12 cells were co-transfected with the pCMV6-empty or pCMV6-SNAI1 vectors and the reporter plasmid carrying the full-length *Fgf21* (−1764) promoter and stimulated with 0.2 µM thapsigargin for 24 h. Luciferase activity was normalized to the Renilla luciferase internal control and expressed as fold change relative to cells co-transfected with the pCMV6-emty vector. Data are the mean and standard deviation from three to six independent experiments and were evaluated using one-way or two-way ANOVA. (C, D) In differentiating myoblasts, IRE1 and PERK inhibition reduce the expression of *Fgf21* and *Atf3* mRNA, respectively. RT-qPCR was performed on RNA extracted from C2C12 cells induced to differentiate for 24 h in presence of 10 µM of the ER stress inhibitors, GSK2656157 (PERK inhibitor), Melatonin (ATF6 inhibitor), and 4µ8C (IRE1 inhibitor). (E) Inhibition of the PERK pathway reduced DDIT3/CHOP expression. C2C12 cells were differentiated for 24 h in DM and whole-cell extracts were used in western blot analysis. (F) Inhibition of IRE1 and ATF6 pathways reduced MYH3 expression. C2C12 cells were differentiated for 48 h in DM and whole-cell extracts were used in western blot analysis.

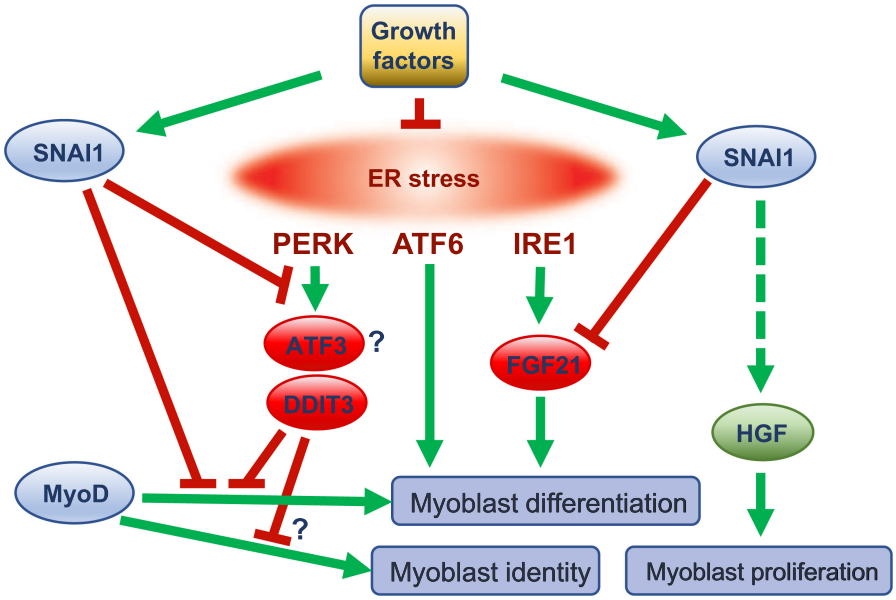

FIGURE 8 Scheme of the regulatory network connecting SNAI1, FGF21, and ER stress in the myoblasts. SNAI1 directly represses *Fgf21* expression that in turn promotes myoblast cell cycle exit and terminal differentiation. SNAI1 also represses the expression of ER stress target genes downstream of the IRE1 sensor and the terminal differentiation program driven by MyoD. HGF expression, consistently with its role in promoting myoblast proliferation, is indirectly activated by SNAI1.

E box in the *Fgf21* promoter, suggesting that their opposite effect on the *Fgf21* transcription is not based on a simple competition for the binding sites. Similarly, we also found that SNAI1 directly binds the *Atf3* promoter. Together, these results underline the complex effects of SNAI1 on gene expression and function during the myoblast proliferation and differentiation programs engaged in responses to muscle injury.

In conclusion, our findings and previous studies support a model wherein SNAI1 can contribute to the undifferentiated phenotype of myoblasts by indirectly promoting the expression of *Hgf* and *Pdgfra* as well as several other pro-proliferative genes while directly repressing the expression of the MyoD target genes involved in myoblast terminal differentiation and the pro-differentiation myokine, FGF21 (Figure 8). As FGF21 is directly involved in myoblast differentiation, we outline a new mechanism by which SNAI1 inhibits myoblast terminal differentiation. We also described that SNAI1 negative regulates the expression of genes such as *Atf3*, *Ddit3/Chop*, and *Hspa5*, which are downstream of the PERK-dependent arm of ER stress. Because DIDT3/CHOP directly repressed the transcription of the MyoD gene,[20] in our model, we speculate that SNAI1 represses DIDT3/CHOP to contribute to the maintenance of myoblast identity and the delicate equilibrium between proliferation and differentiation (Figure 8). Unlike DIDT3/CHOP, less is known about the role of HSPA5 and ATF3 in the terminal differentiation of myoblasts and further studies are necessary to address this issue.

AUTHOR CONTRIBUTIONS

Federico Galvagni conceived and designed the research; Ines Elia, Giulia Realini, Sara Borghi, Vittoria Di Mauro, Laura Bottoni, Salvatore Tornambè, Libero Vitiello, and Francesco Neri performed the research and acquired the data; Federico Galvagni, Salvatore Oliviero, Maurizio Orlandini, Mario Chiariello, Stephen Weiss, Annalaura Tamburrini, and Francesco Neri analyzed and interpreted the data. Salvatore Oliviero, Maurizio Orlandini, Mario Chiariello, Stephen Weiss acquired the funds. All authors were involved in drafting and revising the manuscript.

ACKNOWLEDGMENTS

This study was supported by MIUR (Ministero dell'Istruzione, dell'Università e della Ricerca) grant "Dipartimento di Eccellenza" 2018–2022 to the Department of Biotechnology, Chemistry and Pharmacy grant (F.G. and M.O.). We thank Prof. Cristina Ulivieri for providing us with Thapsigargin.

DISCLOSURES

The authors declare no conflicts of interest.

DATA AVAILABILITY STATEMENT

The data that support the findings of this study are available in the methods and supplementary material of this article.

REFERENCES

1. Galvagni F, Lentucci C, Neri F, et al. Snai1 promotes ESC exit from the pluripotency by direct repression of self-renewal genes. *Stem Cells*. 2015;33:742-750.
2. Martinez-Estrada OM, Culleres A, Soriano FX, et al. The transcription factors Slug and Snail act as repressors of Claudin-1 expression in epithelial cells. *Biochem J*. 2006;394:449-457.
3. Peinado H, Ballestar E, Esteller M, Cano A. Snail mediates E-cadherin repression by the recruitment of the Sin3A/histone deacetylase 1 (HDAC1)/HDAC2 complex. *Mol Cell Biol*. 2004;24:306-319.

4. Soleimani VD, Yin H, Jahani-Asl A, et al. Snail regulates MyoD binding-site occupancy to direct enhancer switching and differentiation-specific transcription in myogenesis. *Mol Cell*. 2012;47:457-468.
5. Markan KR, Naber MC, Ameka MK, et al. Circulating FGF21 is liver derived and enhances glucose uptake during refeeding and overfeeding. *Diabetes*. 2014;63:4057-4063.
6. Izumiya Y, Bina HA, Ouchi N, Akasaki Y, Kharitonenkov A, Walsh K. FGF21 is an Akt-regulated myokine. *FEBS Lett*. 2008;582:3805-3810.
7. Ribas F, Villarroya J, Hondares E, Giralt M, Villarroya F. FGF21 expression and release in muscle cells: involvement of MyoD and regulation by mitochondria-driven signalling. *Biochem J*. 2014;463:191-199.
8. Liu X, Wang Y, Hou L, Xiong Y, Zhao S. Fibroblast Growth Factor 21 (FGF21) promotes formation of aerobic myofibers via the FGF21-SIRT1-AMPK-PGC1alpha pathway. *J Cell Physiol*. 2017;232:1893-1906.
9. Liu X, Wang Y, Zhao S, Li X. Fibroblast Growth Factor 21 promotes C2C12 cells myogenic differentiation by enhancing cell cycle exit. *Biomed Res Int*. 2017;2017:1648715.
10. Zhou S, Qian B, Wang L, Zhang C, Hogan MV, Li H. Altered bone-regulating myokine expression in skeletal muscle of Duchenne muscular dystrophy mouse models. *Muscle Nerve*. 2018;58(4):573-582.
11. Nakanishi K, Sudo T, Morishima N. Endoplasmic reticulum stress signaling transmitted by ATF6 mediates apoptosis during muscle development. *J Cell Biol*. 2005;169:555-560.
12. Nakanishi K, Dohmae N, Morishima N. Endoplasmic reticulum stress increases myofiber formation in vitro. *FASEB J*. 2007;21:2994-3003.
13. He S, Fu T, Yu Y, et al. IRE1alpha regulates skeletal muscle regeneration through Myostatin mRNA decay. *J Clin Invest*. 2021;131(17):e143737.
14. Malhotra JD, Kaufman RJ. The endoplasmic reticulum and the unfolded protein response. *Semin Cell Dev Biol*. 2007;18:716-731.
15. Wu J, Kaufman RJ. From acute ER stress to physiological roles of the unfolded protein response. *Cell Death Differ*. 2006;13(3):374-384.
16. Wang M, Kaufman RJ. The impact of the endoplasmic reticulum protein-folding environment on cancer development. *Nat Rev Cancer*. 2014;14(9):581-597.
17. Hetz C. The unfolded protein response: controlling cell fate decisions under ER stress and beyond. *Nat Rev Mol Cell Biol*. 2012;13(2):89-102.
18. Tan YY, Zhang Y, Li B, et al. PERK signaling controls myoblast differentiation by regulating MicroRNA networks. *Front Cell Dev Biol*. 2021;9:670435.
19. Shi L, Zhou B, Li P, et al. MicroRNA-128 targets myostatin at coding domain sequence to regulate myoblasts in skeletal muscle development. *Cell Signal*. 2015;27(9):1895-1904.
20. Alter J, Bengal E. Stress-induced C/EBP homology protein (CHOP) represses MyoD transcription to delay myoblast differentiation. *PLoS One*. 2011;6(12):e29498.
21. Galvagni F, Cantini M, Oliviero S. The utrophin gene is transcriptionally up-regulated in regenerating muscle. *J Biol Chem*. 2002;277:19106-19113.
22. Yaffe D, Saxel O. Serial passaging and differentiation of myogenic cells isolated from dystrophic mouse muscle. *Nature*. 1977;270:725-727.
23. Galvagni F, Oliviero S. Utrophin transcription is activated by an intronic enhancer. *J Biol Chem*. 2000;275:3168-3172.
24. Anselmi F, Orlandini M, Rocchigiani M, et al. c-ABL modulates MAP kinases activation downstream of VEGFR-2 signaling by direct phosphorylation of the adaptor proteins GRB2 and NCK1. *Angiogenesis*. 2012;15:187-197.
25. Salameh A, Galvagni F, Anselmi F, De Clemente C, Orlandini M, Oliviero S. Growth factor stimulation induces cell survival by c-Jun. ATF2-dependent activation of Bcl-XL. *J Biol Chem*. 2010;285:23096-23104.
26. Haring M, Offermann S, Danker T, Horst I, Peterhansel C, Stam M. Chromatin immunoprecipitation: optimization, quantitative analysis and data normalization. *Plant Methods*. 2007;3:11.
27. Zink W, Graf BM, Sinner B, Martin E, Fink RH, Kunst G. Differential effects of bupivacaine on intracellular Ca^{2+} regulation: potential mechanisms of its myotoxicity. *Anesthesiology*. 2002;97:710-716.
28. Zheng H, Shen M, Zha YL, et al. PKD1 phosphorylation-dependent degradation of SNAIL by SCF-FBXO11 regulates epithelial-mesenchymal transition and metastasis. *Cancer Cell*. 2014;26(3):358-373.
29. Kleger A, Loebnitz C, Pusapati GV, et al. Protein kinase D2 is an essential regulator of murine myoblast differentiation. *PLoS One*. 2011;6(1):e14599.
30. Peiró S, Escrivà M, Puig I, et al. Snail1 transcriptional repressor binds to its own promoter and controls its expression. *Nucleic Acids Res*. 2006;34(7):2077-2084.
31. Huang da W, Sherman BT, Lempicki RA. Systematic and integrative analysis of large gene lists using DAVID bioinformatics resources. *Nat Protoc*. 2009;4:44-57.
32. Supek F, Bosnjak M, Skunca N, Smuc T. REVIGO summarizes and visualizes long lists of gene ontology terms. *PLoS One*. 2011;6:e21800.
33. Edagawa M, Kawauchi J, Hirata M, et al. Role of activating transcription factor 3 (ATF3) in endoplasmic reticulum (ER) stress-induced sensitization of p53-deficient human colon cancer cells to tumor necrosis factor (TNF)-related apoptosis-inducing ligand (TRAIL)-mediated apoptosis through up-regulation of death receptor 5 (DR5) by zerumbone and celecoxib. *J Biol Chem*. 2014;289:21544-21561.
34. Wan XS, Lu XH, Xiao YC, et al. ATF4- and CHOP-dependent induction of FGF21 through endoplasmic reticulum stress. *Biomed Res Int*. 2014;2014:807874.
35. Schaap FG, Kremer AE, Lamers WH, Jansen PL, Gaemers IC. Fibroblast growth factor 21 is induced by endoplasmic reticulum stress. *Biochimie*. 2013;95:692-699.
36. Guardiola O, Andolfi G, Tirone M, Iavarone F, Brunelli S, Minchiotti G. Induction of acute skeletal muscle regeneration by cardiotoxin injection. *J Vis Exp*. 2017;119:54515.
37. Seale P, Ishibashi J, Holterman C, Rudnicki MA. Muscle satellite cell-specific genes identified by genetic profiling of MyoD-deficient myogenic cell. *Dev Biol*. 2004;275:287-300.
38. Miller KJ, Thaloor D, Matteson S, Pavlath GK. Hepatocyte growth factor affects satellite cell activation and differentiation

in regenerating skeletal muscle. *Am J Physiol Cell Physiol*. 2000;278:174-C181.

39. Leshem Y, Spicer DB, Gal-Levi R, Halevy O. Hepatocyte growth factor (HGF) inhibits skeletal muscle cell differentiation: a role for the bHLH protein twist and the cdk inhibitor p27. *J Cell Physiol*. 2000;184:101-109.
40. Anastasi S, Giordano S, Sthandier O, et al. A natural hepatocyte growth factor/scatter factor autocrine loop in myoblast cells and the effect of the constitutive met kinase activation on myogenic differentiation. *J Cell Biol*. 1997;137:1057-1068.
41. Contreras O, Cordova-Casanova A, Brandan E. PDGF-PDGFR network differentially regulates the fate, migration, proliferation, and cell cycle progression of myogenic cells. *Cell Signal*. 2021;84:110036.
42. Shan T, Xu Z, Wu W, Liu J, Wang Y. Roles of Notch1 signaling in regulating satellite cell fates choices and postnatal skeletal myogenesis. *J Cell Physiol*. 2017;232:2964-2967.
43. Lee NK, Skinner JP, Zajac JD, MacLean HE. Ornithine decarboxylase is upregulated by the androgen receptor in skeletal muscle and regulates myoblast proliferation. *Am J Physiol Endocrinol Metab*. 2011;301:172-E179.
44. Kitzmann M, Vandromme M, Schaeffer V, et al. cdk1- and cdk2-mediated phosphorylation of MyoD Ser200 in growing C2 myoblasts: role in modulating MyoD half-life and myogenic activity. *Mol Cell Biol*. 1999;19:3167-3176.
45. Correra RM, Ollitrault D, Valente M, et al. The imprinted gene Pw1/Peg3 regulates skeletal muscle growth, satellite cell metabolic state, and self-renewal. *Sci Rep*. 2018;8:14649-x.
46. Bengal E, Ransone L, Scharfmann R, et al. Functional antagonism between c-Jun and MyoD proteins: a direct physical association. *Cell*. 1992;68:507-519.
47. El Haddad M, Notarnicola C, Evano B, et al. Retinoic acid maintains human skeletal muscle progenitor cells in an immature state. *Cell Mol Life Sci*. 2017;74:1923-1936.
48. Li H, Sun H, Qian B, et al. Increased expression of FGF-21 negatively affects bone homeostasis in dystrophin/utrophin double knockout mice. *J Bone Miner Res*. 2020;35:738-752.
49. Morville T, Sahl RE, Trammell SA, et al. Divergent effects of resistance and endurance exercise on plasma bile acids, FGF19, and FGF21 in humans. *JCI Insight*. 2018;3(15):e122737.
50. Sun H, Sherrier M, Li H. Skeletal muscle and bone - emerging targets of Fibroblast Growth Factor-21. *Front Physiol*. 2021;12:625287.
51. Yu Y, He J, Li S, et al. Fibroblast growth factor 21 (FGF21) inhibits macrophage-mediated inflammation by activating Nrf2 and suppressing the NF-kappaB signaling pathway. *Int Immunopharmacol*. 2016;38:144-152.
52. Li H, Wu G, Fang Q, et al. Fibroblast growth factor 21 increases insulin sensitivity through specific expansion of subcutaneous fat. *Nat Commun*. 2018;9:272-279.
53. Contreras-Shannon V, Ochoa O, Reyes-Reyna SM, et al. Fat accumulation with altered inflammation and regeneration in skeletal muscle of CCR2−/− mice following ischemic injury. *Am J Physiol Cell Physiol*. 2007;292:953-C967.
54. Shireman PK, Contreras-Shannon V, Ochoa O, Karia BP, Michalek JE, McManus LM. MCP-1 deficiency causes altered inflammation with impaired skeletal muscle regeneration. *J Leukoc Biol*. 2007;81:775-785.
55. Summan M, Warren GL, Mercer RR, et al. Macrophages and skeletal muscle regeneration: a clodronate-containing liposome depletion study. *Am J Physiol Regul Integr Comp Physiol*. 2006;290:1488-R1495.
56. Pimorady-Esfahani A, Grounds MD, McMenamin PG. Macrophages and dendritic cells in normal and regenerating murine skeletal muscle. *Muscle Nerve*. 1997;20:158-166.
57. McLennan IS. Degenerating and regenerating skeletal muscles contain several subpopulations of macrophages with distinct spatial and temporal distributions. *J Anat*. 1996;188(Pt 1):17-28.
58. Bencze M, Negroni E, Vallese D, et al. Proinflammatory macrophages enhance the regenerative capacity of human myoblasts by modifying their kinetics of proliferation and differentiation. *Mol Ther*. 2012;20:2168-2179.
59. Arnold L, Henry A, Poron F, et al. Inflammatory monocytes recruited after skeletal muscle injury switch into antiinflammatory macrophages to support myogenesis. *J Exp Med*. 2007;204:1057-1069.
60. Wek RC, Jiang HY, Anthony TG. Coping with stress: eIF2 kinases and translational control. *Biochem Soc Trans*. 2006;34:7-11.
61. Ku HC, Cheng CF. Master regulator activating transcription factor 3 (ATF3) in metabolic homeostasis and cancer. *Front Endocrinol (Lausanne)*. 2020;11:556.
62. Luo S, Baumeister P, Yang S, Abcouwer SF, Lee AS. Induction of Grp78/BiP by translational block: activation of the Grp78 promoter by ATF4 through and upstream ATF/CRE site independent of the endoplasmic reticulum stress elements. *J Biol Chem*. 2003;278:37375-37385.

SUPPORTING INFORMATION

Additional supporting information may be found in the online version of the article at the publisher's website.

How to cite this article: Elia I, Realini G, Di Mauro V, et al. SNAI1 is upregulated during muscle regeneration and represses FGF21 and ATF3 expression by directly binding their promoters. *The FASEB Journal*. 2022;36:e22401. https://doi.org/10.1096/fj.202200215R